Thermochimica Acta 373 (2001) 37–43

thermochimica acta

www.elsevier.com/locate/tca

Thermal analysis of La–Ba oxalate and role of γ-irradiation there on

H. Nayak*, D. Bhatta

Department of Chemistry, Utkal University, Bhubaneswar 751004, India

Received 7 September 2000; accepted 10 January 2001

Abstract

Lanthanum–barium oxalate was prepared and characterised by chemical and thermal analysis, X-ray diffraction and plasma emission spectroscopy. X-ray analysis showed the presence of a uniphase system. The kinetics of decomposition of oxalates of La and Ba as well as coprecipitated La–Ba oxalate have been investigated in air using dynamic thermogravimetry. The decomposition of mixed oxalate occurred with two over-lapping exotherms, corresponding to the decomposition of lanthanum oxalate followed by that of barium.

The kinetics of decomposition of the irradiated salt was studied over the same temperature range as that of the unirradiated one in air and activation energies obtained from the slopes of Coat–Redfern's plot. Kinetic analyses following various theoretical models of solid state reactions showed that the best fit was obtained for a third order reaction and geometrical models. It was evident that though there was increase in the activation energy as well as frequency factor with increasing radiation dose, reverse phenomenon takes place in the case of reaction rate. The effect of γ-irradiation on the process and the mechanism involved therein has been discussed. © 2001 Elsevier Science B.V. All rights reserved.

Keywords: γ-Irradiation; La–Ba oxalate; X-ray diffraction

1. Introduction

The preparation of La–Ba oxalate, constitutes a part of the oxalate precursor synthesis of bulk La $Ba_{2-x}Cu_{3-x}$ $Co_xO_{7-\delta}$, $La_{2-x}Ba_xSrCu_2O_6$ and $LaBa_2$ $Cu_3O_{7-\delta}$ superconductors by coprecipitation filtration techniques [1,2]. Various chemical routes such as sol–gel [3], spray drying [4] and coprecipitation have been carried out in order to improve the homogeniety of the precursors and consequently the properties of superconducting materials. The oxalate ion being the most used precipitating agent [5] has received much attention in synthesising superconducting double or multicomponent oxides [6] as well as high purity titanates, stanates, ferrites and zirconates of prefect stoichiometry. Synthesis and thermal decomposition of double oxalates of rare earths(III) with lithium, sodium, potassium, rubidium, caesium and ammonium has already been reported [7]. Transition metals with approximately same ionic radii form solid solutions by coprecipitation of their oxalates [8]. Decomposition of alkaline earth–copper oxalates leads to formation of high purity metal cuprates [9]. It has been reported [6] that during decomposition of alkaline earth metal oxalates doped with rare earths(III), the component oxalates retain their identity in the mixed oxalates, e.g. in coprecipitated calcium–lanthanum oxalate the single decomposition exotherm splits into three peaks at 365, 395 and

---

[*] Corresponding author.

0040-6031/01/$ – see front matter © 2001 Elsevier Science B.V. All rights reserved.
PII: S0040-6031(01)00446-4

400°C, respectively, indicating a remarkable decrease in the decomposition temperature of pure calcium oxalate which occurs at 460°C. Decomposition of various ternary mixture of oxalates of La(III), Ba(II) and Cu(II) has already been studied adopting TG, DTA and XRD techniques [10]. Kinetic studies of the coprecipitated Y–Ba–Cu oxalate show a significant deviation in thermodynamic parameters from that of the constituent pure salts [11]. Thermal decomposition of citrates and tartarates of rare earths, alkali and alkaline earth metals, and transition metals have been reported by many workers [12–14]. The present work throws light on the thermal analysis of coprecipitate and mechanical mixture of La–Ba oxalate in order to explore the suitable ratio, La/Ba for preparing superconducting phases. Kinetic analysis of the non-isothermal data on the decomposition of mixture is carried out using various solid state reaction models and integral method of dynamic data analysis.

2. Experimental

The chemicals and reagents used were AR grade. The required amounts of $Ba(NO_3)_2$ and $La(NO_3)_3$ (1:1 mole ratio) were dissolved in dilute HNO_3 (J.T. Baker) and the pH of the solution was maintained at 3–3.5. Diethyl oxalate was added and digested for 2 h. The compound was precipitated from the hot solution by addition of 4% (w/v) oxalic acid. The solution was digested for 1 h on a water bath, filtered, washed with distilled water and dried.

Compositional analysis of the samples was carried out by chemical methods. The La–Ba stoichiometry in the coprecipitate was determined by inductively coupled plasma–atomic emission spectroscopy (ICP-AES, Perkin-Elmer p-400).

The crystals of uniform mesh size were exposed to different doses, 0.15–0.25 MGy of ^{60}Co γ-rays at room temperature and TG-DTA data of unirradiated and irradiated samples were recorded at the heating rate of 4°C $\min^{-1}$ in air, using a Schimadzu DTG-50 thermal analysis unit and the samples were pyrolised upto 550°C. TGA data of the physical mixture of lanthanum and barium oxalate was carried out in order to compare the data with that of the coprecipitate.

3. Results and discussion

3.1. Thermal analysis

Decomposition of anhydrous barium oxalate occurred at 450–480°C with an exotherm in static air. But in case of the La–Ba coprecipitate, three different exotherms at 387, 405 and 440°C were obtained (Fig. 1(b)) indicating the formation of an intermediate during the decomposition or the occurrence of the process in three different stages which is not obtained in the case of mechanical mixture. Exotherm at 387°C may be due to the formation of an intermediate $La_2(C_2O_4)\ (CO_3)_2$, suggesting that reaction started at a higher temperature compared to that of $La_2(C_2O_4)_3$ which took place at 382°C (Fig. 1(a)).

3.2. XRD analysis

The presence of a prominent lanthanide peak along with barium (Table 1) in the XRD diffraction patterns suggests the formation of coprecipitate. Presence of Ba^{2+} in the lanthanum oxalate hydrate lattice results in a shift in the diffraction lines ($d = 3.2536$) of the latter to higher 2θ angle. It is evident from this that the structure of the coprecipitate is different from that of the $La_2(C_2O_4)_3$, 10 H_2O. The decrease in cell volume may arise from the partial substitution of La^{3+} (1.08 Å) by Ba^{2+} (1.48 Å) in the lattice of the former. Additional phases are detected in which the diffraction lines are shifted to lower 2θ angles compared to the lattice of BaC_2O_4.

3.3. Kinetic analysis

Programmed- and weightloss-temperature plot were redrawn as fractional decomposition, α versus temperature, T (Fig. 2), from which differential curves ($d\alpha/dT$) versus T were obtained (Fig. 3) there indicated that the coprecipitate was significantly different from that of the mechanical mixture. The weightloss data between the temperature range, 380–500°C (Table 2) only was considered. This showed an increase in fractional decomposition, α for La–Ba oxalate, compared to that of lanthanum oxalate. At lower temperatures, 380–400°C, the reaction was third order law (F_3) with $\alpha < 0.3$, leading to separation into component

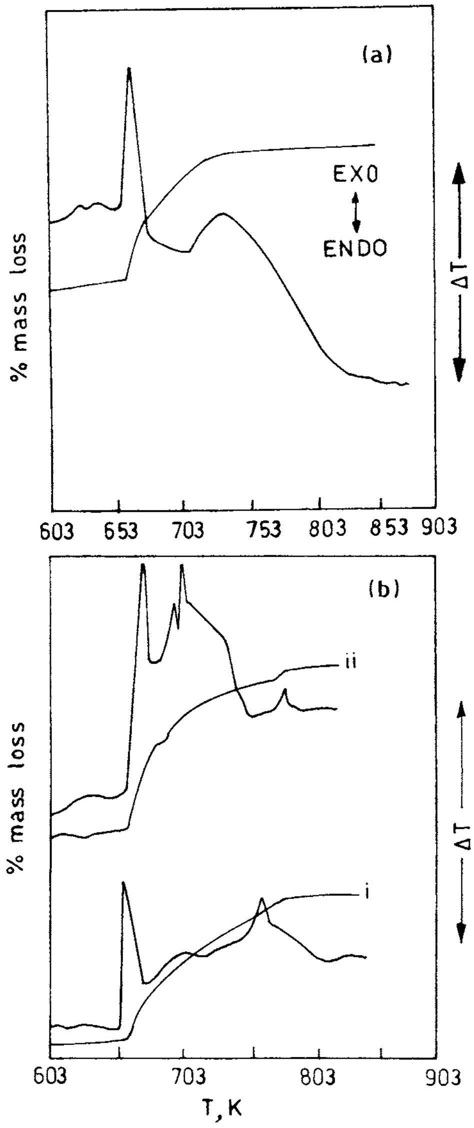

Fig. 1. TG and DTA curves for (a) La oxalate and (b) coprecipitated La–Ba oxalate and mechanical mixture of La and Ba oxalate at heating rate of 4°C min^{-1} in air.

oxalate and partial decomposition of lanthanum oxalate to intermediate $La_2(C_2O_4)$ $(CO_3)_2$. But at higher temperature, 410–490°C the "α–T" curves corresponded to a contracting volume equation (R_3). As the decomposition temperatures of consituent oxalates were different, (Fig. 4) it was difficult to study the kinetics of individual breakdown steps. Thus, an overall kinetic study of the oxalate breakdown steps has been carried out. The decomposition process follows two stages, acceleratory (380–400°C) and decay (410–490°C).

Table 1
XRD data of coprecipitated and pure oxalates

d-values	
La oxalate	La–Ba oxalate
5.2668	3.2665
3.7802	2.7904
3.2536	2.3805
2.4248	2.1439
1.9839	1.9382
1.8957	1.9277

Kinetic analysis of different steps in TG, resulted in activation energies of 170 ± 5 and 33 ± 5 kJ mol^{-1}, for the acceleratory and decay stages, respectively, which are higher than that of the individual salt (Table 3).

Upon irradiation, the activation energy increased marginally (Table 4) but increased with increasing radiation dose for both the stages. Kinetic parameters were determined in the specified temperature ranges using Coat–Redfern's equation

$$\log\frac{g(\alpha)}{T^2} = \log\frac{AR}{\beta E} - \frac{E}{2.303RT} \qquad (1)$$

where A is the pre-exponential factor, R the universal gas constant, β the rate of heating, E the energy of activation, T the absolute temperature. $g(\alpha)$ was chosen for various rate determining mechanisms for both the periods. $\log[g(\alpha)/T^2]$ was calculated for each

Table 2
Variation of fractional decomposition, α with temperature 'T' for La oxalate and coprecipitated La–Ba oxalate in the temperature range 653–773 K

T (K)	Fractional decomposed, α	
	La oxalate	La–Ba oxalate
653	0.049	0.050
673	0.364	0.451
693	0.557	0.650
713	0.674	0.770
733	0.787	0.846
753	0.841	0.905
773	0.913	0.950

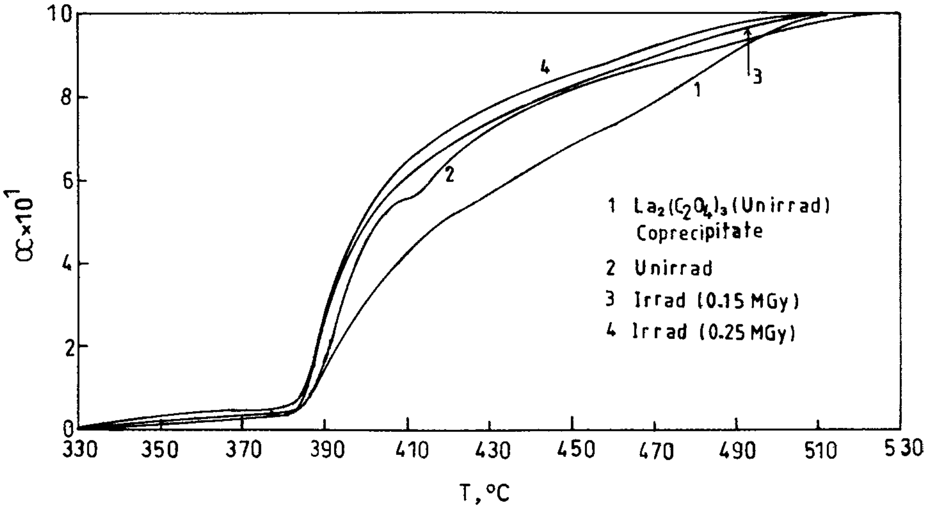

Fig. 2. Variation of fractional decomposition, α with temperature *T*, in the range 653–773 K.

possible rate controlling mechanism and plotted against 1/*T* (Figs. 5 and 6). The linearity of the plot was observed by best fitting the data to the highest coefficient of linear regression analysis.

The data on unirradiated and irradiated salts (Table 4) indicate that activation energy of the mixed crystal is higher than that of the individual one which may arise due to stronger bond (C–OM) in the case of former. Once the bond is broken, the reaction proceeds at a detectable rate and is higher than that of the lanthanum oxalate, in the temperature range, 380–400°C which is different from that of the barium oxalate. The activation energy follows an increasing trend in case of irradiated salt for the acceleratory stage, but deviation is observed for decay period. There is an initial decrease in activation energy at lower doses and the reverse phenomenon occurs at higher one. The higher energy of activation for the acceleratory period may be attributed to cage effect. At higher doses the damaged entities encapsulate the host nuclei and act as barrier for further decomposition to proceed.

In case of decay period, there is decrease in activation energy at lower doses which may arise due to partial weakening of the La–Ba–metal oxalate bonds

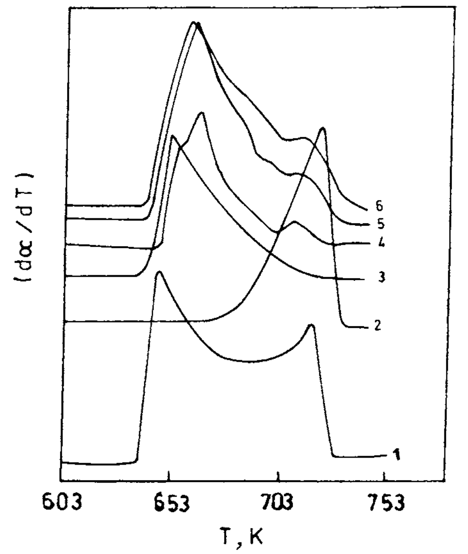

Fig. 3. DTG curves of samples: (1) mechanical mixture of La and Ba oxalate; (2) Ba oxalate; (3) La oxalate; (4) La–Ba oxalate; (5) La–Ba oxalate (0.15 MGy); (6) La–Ba oxalate (0.25 MGy).

Table 3
Activation energies of decomposition of oxalates of La and Ba and coprecipitated La–Ba oxalate in air[a]

	Activation energy E (±5) (kJ mol^{-1})	Correlation coefficient, r
Lanthanum oxalate	146.20	0.9892
Barium oxalate	165.03	0.9989
Coprecipitated La–Ba oxalate	170.30	0.9798

[a] E derived for acceleratory stages.

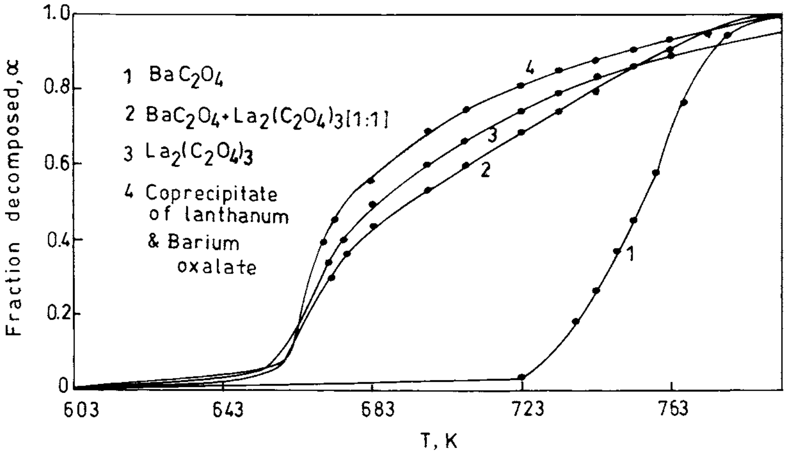

Fig. 4. Comparision of decomposition characteristics of various samples.

but the higher values obtained at higher doses may be attributed to encapsulation resulted due to residual carbon.

The rate constant 'k' in case of coprecipitate follows the same trend as that of the activation energy, and the increase is marginal with increasing radiation dose. Positive values of entropy changes (ΔS), in case of irradiated material indicate a faster reaction and less ordered activated complex compared to unirradiated sample. A knowledge of 'A' enables the evaluation of (ΔS) and vice versa as has been shown by earlier work [15].

3.4. Role of Irradiation

Upon irradiation with ^{60}Co γ-rays, the Compton effect has the largest cross section except for materials of very high atomic number and more over, the number of atoms displaced has its maximum in the very light elements and diminished to zero at around at. wt 125. Irradiation with these rays, therefore, excludes the possibility of displacements of La (at. wt 138.9) and Ba (at. wt 137.7) by Compton electrons and generates new potential nucleation centres which favours the heterogeneous process. Irradiation enhances the rate as well as the extent of decomposition which may be ascribed to increased penetration or growth. Upon exposure of oxalate to γ-ray vacancies are created in the lattice as

$$La_2(C_2O_4)_3 \overset{\gamma\text{-irradiated}}{\rightleftharpoons} La_2(C_2O_{4-n}\square n) + 3nO \tag{2}$$

where '$\square$' refers to a oxygen vacancy and n is the number of oxygen vacancies.

According to Eq. (2) the number of vacancies produced in the lattice increase with increasing

Table 4
Kinetic parameters for best fit mechanism for the decomposition of unirradiated and irrad. La–Ba oxalate using Coat–Redfern's method

Reaction	T_s (K)	Sample (La–Ba oxalate)	Mechanism	E (±5) (kJ mol^{-1})	log A (S^{-1})	k (±0.05) (S^{-1})	ΔS(± 3) (kJ mol^{-1} K^{-1})
Stage I (653–673 K)	667	Unirradiated	F_3	170.30	13.383	0.3101	4.59
	664	0.15 MGy		200.69	15.410	0.3862	43.43
	660	0.25 MGy		204.45	15.710	0.397	49.20
Stage II (683–763 K)	690	Unirradiated	R_3	33.30	0.973	0.037	−233.27
	713	0.15 MGy		29.20	0.650	0.0345	−239.3
	738	0.25 MGy		37.00	1.320	0.045	−227.17

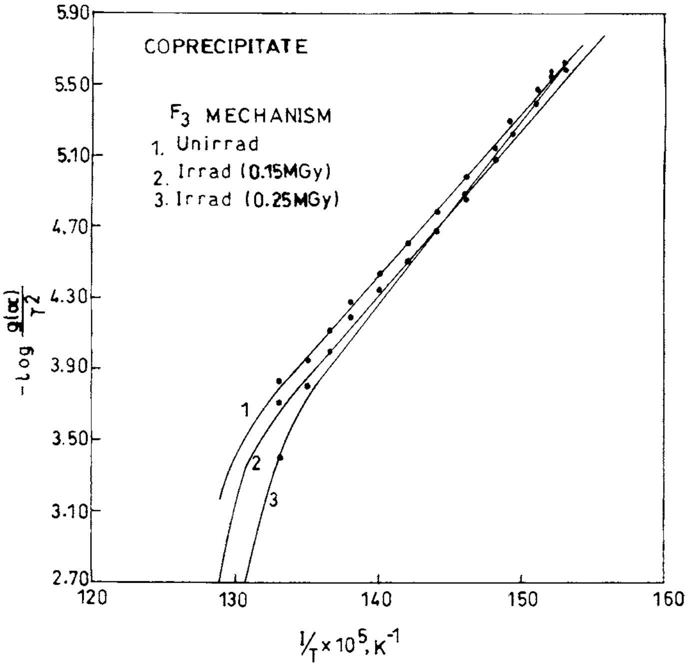

Fig. 5. Variation of log[$g(\alpha)/T^2$] with $1/T$ using the rate controlling mechanism F_3.

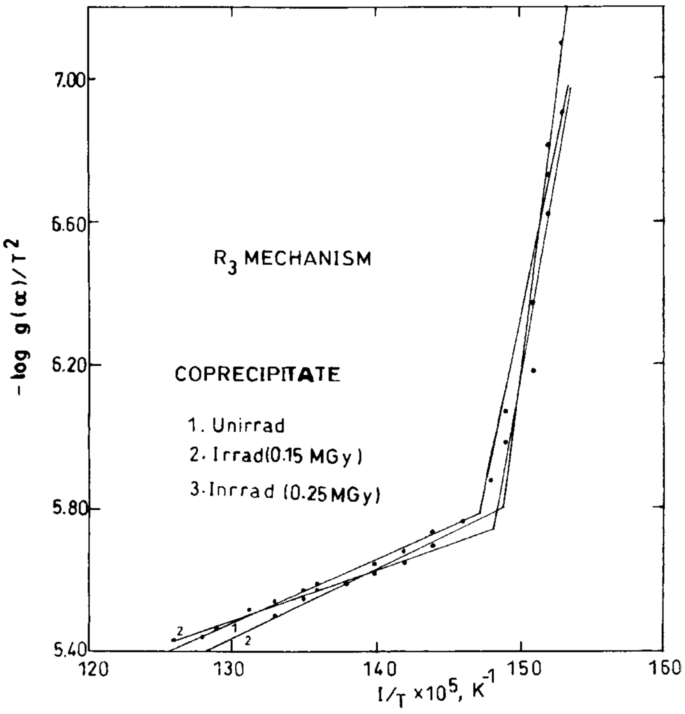

Fig. 6. Variation of log[$g(\alpha)/T^2$] with $1/T$ using the R_3 reaction mechanism.

radiation dose. These generate additional potential nucleation centres and facilitates the decomposition at lower doses, but at higher dosages, crystal defects (radiation damage) are generated and there is formation of unreactive radicals and centres inside the crystals [16], resulting in a decrease in the number of decomposition centres, hence, the effect is not of much significance. Upon irradiation with γ-rays, apart from trapped electrons (e^-) and holes (h^+) there will be atoms, radicals and ions in the interstitial positions where as the fragments bearing the same charge as the parent ion will be in the lattice position of the later. These damaged species constitute decomposition nuclei themselves and may be termed as irradiation nuclei 'n_i' which increase in size and number with increasing radiation dose [17]. Due to increasing number of point defects and additional nucleation centres, sufficient strain is created in the lattice to fratcture the crystal, thus, generating new reactive centres, accelerating the decomposition process.

Acknowledgements

Financial support by the C.S.I.R., New Delhi is gratefully acknowledged.

References

[1] D.W. Johnson, P.K. Gallagher, Ceramic Processing Before Firing, Wiley, New York, 1978, p. 125.
[2] A. Vos, J. Mullens, R. Carleer, J. Yperman, J. Vanhees, L.C. Van Poucke, J. Therm. Anal. 40 (1993) 303.
[3] M.K. Van Bael, J. Mullens, R. Nouwen, J. Yperman, L.C. Van Poucke, J. Therm. Anal. 48 (1997) 989.
[4] S. Hoste, H. Vlaeminck, P.H. De Ryck, F. Persyn, R. Mouton, G.P. Van Der Kelen, Supercond. Sci. Technol. 1 (1989) 239.
[5] A. Vos, J. Mullens, R. Carleer, J. Yperman, L.C. Van Poucke, Bull. Soc. Chim. Belg. 101 (1992) 187.
[6] U. Patnaik, J. Muralidhar, Thermochim. Acta 274 (1996) 261.
[7] O. Gencova, J. Siftar, J. Therm. Anal. 48 (1997) 321.
[8] X. Gao, D. Chen, D. Dollimore, E. Skrzypczak-Jankum, P. Burckel, Thermochim. Acta 220 (1993) 75.
[9] M. Insausti, R. Cortes, M.I. Arriortua, T. Rojo, E.H. Bocaregra, Solid State Ionics 63 (1993) 351.
[10] L. Bapat, G.N. Natu, M. Bhide, J. Kher, J. Therm. Anal. 48 (1997) 819.
[11] C.K. Hsu, J.S. Lee, C.W. Huang, J. Therm. Anal. 51 (1998) 295.
[12] V.K. Sankarnarayanan, N.S. Gajbhiye, Thermochim. Acta 153 (1989) 337.
[13] N.S. Gajbhiye, A. Vijayalakshmi, J. Therm. Anal. 51 (1998) 517.
[14] N.A. Baranov, V.B. Okhotnikov, A.K. Galway, G.M. Laverty, Solid State Ionics 43 (1990) 37.
[15] A.S. Gopalkrishnamurty, M. Subha, R. Narayanan-kutty, J. Inorg. Nucl. Chem. 37 (1975) 891.
[16] M.M.M. Ebd EI-Wahab, R.M. Mahfoud, Thermochim. Acta 274 (1996) 281.
[17] S. Patnaik, D. Bhatta, Radiochim. Acta 73 (1996) 21.